

Simultaneous Detection of Glutathione and Hydrogen Polysulfides from Different Emission Channels

Wenqiang Chen, Xiuxiu Yue, Hui Zhang, Wenxiu Li, Liangliang Zhang, Qi Xiao, Chusheng Huang, Jiarong Sheng, and Xiangzhi Song

Anal. Chem., **Just Accepted Manuscript** • DOI: 10.1021/acs.analchem.7b04033 • Publication Date (Web): 03 Nov 2017

Downloaded from <http://pubs.acs.org> on November 4, 2017

Just Accepted

“Just Accepted” manuscripts have been peer-reviewed and accepted for publication. They are posted online prior to technical editing, formatting for publication and author proofing. The American Chemical Society provides “Just Accepted” as a free service to the research community to expedite the dissemination of scientific material as soon as possible after acceptance. “Just Accepted” manuscripts appear in full in PDF format accompanied by an HTML abstract. “Just Accepted” manuscripts have been fully peer reviewed, but should not be considered the official version of record. They are accessible to all readers and citable by the Digital Object Identifier (DOI®). “Just Accepted” is an optional service offered to authors. Therefore, the “Just Accepted” Web site may not include all articles that will be published in the journal. After a manuscript is technically edited and formatted, it will be removed from the “Just Accepted” Web site and published as an ASAP article. Note that technical editing may introduce minor changes to the manuscript text and/or graphics which could affect content, and all legal disclaimers and ethical guidelines that apply to the journal pertain. ACS cannot be held responsible for errors or consequences arising from the use of information contained in these “Just Accepted” manuscripts.



Simultaneous Detection of Glutathione and Hydrogen Polysulfides from Different Emission Channels

Wenqiang Chen,^{**†} Xiuxiu Yue,[†] Hui Zhang,[§] Wenxiu Li,[‡] Liangliang Zhang,[‡] Qi Xiao,[†] Chusheng Huang,[†] Jiarong Sheng,^{**†} and Xiangzhi Song[§]

[†]College of Chemistry and Materials Science, Guangxi Teachers Education University, 530001 Nanning, Guangxi, P. R. China.

[‡]State Key Laboratory for the Chemistry and Molecular Engineering of Medicinal Resources of Education Ministry, Guangxi Normal University, 541004 Guilin, Guangxi, P. R. China.

[§]College of Chemistry & Chemical Engineering, Central South University, Changsha, Hunan 410083, P. R. China.

*Corresponding author, E-mail: chenwq@csu.edu.cn; Fax: +86-771-3908065; E-mail: shengjiarong99@163.com; Fax: +86-771-3908018

ABSTRACT: Glutathione (GSH) and hydrogen polysulfides (H_2S_n) play crucial roles in many physiological processes. To unravel the complicated interrelationship and cellular cross-talk between GSH and H_2S_n , the development of single-molecule fluorescent probes that can selectively sense GSH and H_2S_n simultaneously from different emission channels is highly desirable. In this report, we have developed the first dual-detection fluorescent probe, ACC-SePh, which responded to GSH with green fluorescence emission, whereas it reacted with H_2S_n and emitted blue fluorescence. The probe exhibited excellent selectivity and sensitivity toward GSH and H_2S_n over other common reactive sulfur species, such as Cys, Hcy and H_2S . Importantly, we also demonstrated that ACC-SePh can be used for dual-channel imaging of endogenous GSH and H_2S_n in living RAW264.7 cells.

INTRODUCTION SECTION

Given that reactive sulfur species (RSS) play crucial roles in a variety of physiological and pathological processes, an important and ever-increasing research field which focused on the chemical biology of RSS was emerged in recent decades.¹⁻³ Among RSS, glutathione (GSH) is most abundant in the biological system,⁴ functioning as an essential role in maintaining redox homeostasis, and defending against free radicals and toxins.⁵⁻⁶ Aberrant GSH levels in living systems are closely associated with various diseases such as cancer, Alzheimer's disease, Parkinson disease, AIDS, osteoporosis and cardiovascular disease.⁷⁻⁸ Very recently, disentangling the redox biology of hydrogen polysulfides (H_2S_n , $n \geq 2$) has become the current intense interest in RSS.⁹⁻¹² Increasing evidences suggest that H_2S_n exhibit high potency in modulating various physiological processes including activating ion channels, transcription factors and tumor suppressors.⁹⁻¹³

Due to the significance of GSH and H_2S_n in redox biology, establishment of convenient detection methods for these species are highly desirable.¹⁴⁻¹⁶ Unfortunately, the selective detection of GSH over cysteine (Cys) or homocysteine (Hcy) was a great challenge, and as far as we know, merely few examples were reported. One appealing strategy, reported by Yang *et al.*, is based on the distinct reaction processes between GSH, Cys/Hcy and chlorinated BODIPYs, thereby enabling the highly selective detection of GSH over Cys/Hcy.¹⁷ Similarly, fluorescent probes specific for H_2S_n over other RSS are also rare. Pioneered by Xian's group, the first fluorescent probe for H_2S_n was developed by taking advantage of H_2S_n -mediated benzodithione formation.¹⁸ From then on, some more

specific fluorescent probes for H_2S_n were developed based on the extended version of this strategy.¹⁹⁻³⁰

With the in-depth study of the biological pathways of GSH and H_2S_n , growing evidences have indicated that these two species were interrelated in biological systems. For example, endogenous H_2S_n were produced enzymatically by cystathionine- γ -lyase (CSE) and cystathionine β -synthase (CBS),³¹ and GSH might be the actual sulfur source of H_2S_n . Because high levels of H_2S_n precursors, glutathione hydropersulfide ($>100 \mu M$), were detected in the plasma, cells, and tissues of mammals.³² To make sense of the mutual relationship and cellular cross-talk between GSH and H_2S_n , the development of fluorescent probes that can sense GSH and H_2S_n from distinct emission channels is highly valuable. To meet the abovementioned requirements, a simple solution is to use two specific probes simultaneously in a cell.³³⁻³⁴ However, just as pointed out by Suzuki and co-workers, this strategy suffers from limitations such as 1) larger invasive effects, 2) potential cross-talk between different probes, 3) the complicated scenario caused by the distinct localization and metabolisms of the probes.³⁵ Therefore, a single-molecule fluorescent probe that can selectively visualize GSH and H_2S_n simultaneously from different emission channels is desperately needed. To the best of our knowledge, such a single-molecule probe has not been reported yet. Herein, we present the rational design, synthesis and spectral properties of ACC-SePh, the first single-molecule fluorescent probe, which can simultaneously detect GSH and H_2S_n from different emission channels. Significantly, with the help of a laser confocal microscope, we have demonstrated that ACC-SePh was capable of detecting endogenous GSH

and H₂S_n simultaneously in living RAW264.7 cells through dual-color fluorescence imaging.

EXPERIMENTAL SECTION

Materials and instruments

Unless otherwise noted, all reagents were obtained from commercial suppliers and used without further purification. Solvents were purified by standard methods prior to use. Twice-distilled water was used throughout all experiments. NMR spectra were recorded on a BRUKER 300 and 600 spectrometer using TMS as an internal standard. All accurate mass spectrometric experiments were performed on a Xevo G2 QTof MS (Waters, USA). UV-Vis absorption spectra were recorded on a TU-1901 (Puxi, P.R. China) spectrophotometer. Fluorescence spectra were recorded at room temperature using a HITACHI F-4600 fluorescence spectrophotometer with both the excitation and emission slit widths set at 5.0 nm. Cell imaging was performed with a Zeiss LSM 710 laser scanning confocal microscope. TLC analysis was performed on silica gel plates and column chromatography was conducted using silica gel (mesh 200-300), both of which were obtained from Qingdao Ocean Chemicals, China.

General procedure for spectral measurements

A stock solution of ACC-SePh was prepared at 1 mM in DMF. Solutions of various testing species were prepared from Na₂S₂, glutamate (Glu), proline (Pro), serine (Ser), tyrosine (Tyr), glutathione (GSH), cysteine (Cys), methionine (Met), Na₂S, NaHSO₃, Na₂SO₄, Na₂S₂O₃, NaClO, H₂O₂, CaCl₂, MgCl₂, KCl and ZnCl₂ in twice-distilled water. Homocysteine (Hcy) was prepared in PBS buffer (10 mM, pH = 7.4). A typical test solution (10.0 mL) was prepared by placing 0.05 mL of ACC-SePh (1 mM), 5.0 mL of PB buffer (20 mM, pH = 7.4, containing 2 mM CTAB), and an appropriate aliquot of each analyte stock solution into an appropriate amount of twice-distilled water. The resulting solution was shaken well and kept at room temperature (25°C) for 60 min before recording its spectra.

Cell culture and fluorescence imaging

RAW264.7 cells were seeded in a 6-well plate in Dulbecco's modified Eagle's medium (DMEM) supplemented with 10% fetal bovine serum and 1% penicillin. The cells were incubated under an atmosphere of 5% CO₂ and 95% air at 37°C for 24 h. Cell imaging was performed with a Zeiss LSM 710 laser scanning confocal microscope. Before each experiment, cells were washed with PBS buffered solution 3 times. Excitation wavelength: 405 nm. Emissions were collected at 440-460 nm for blue channel and 520-560 nm for green channel.

Synthesis of compound 2

Resorcin (7.609g, 69 mmol) and compound 1 (965 mg, 3.5 mmol) were dissolved in 6 mL of acetonitrile, the mixture was stirred at 0°C for 5 min. Then, a portion of NaClO₂ (1.470 g, 12.25 mmol) and NaH₂PO₄ (1.418 g, 15.75 mmol) (dissolved in 1.5 mL water) was added dropwise to the mixture at 0°C. The reaction mixture was stirred at 0°C for additional 30 min, poured into ice water (30 mL). After acidification of the mixture by 1M HCl, a large amount of yellow precipitates formed. The precipitates were collected by filtration and rinsed with cold water (2×20 mL) and dried under vacuum to afford a

yellow solid (790 mg, 77% yield). Mp: 180-182°C. ¹H NMR (300 MHz, DMSO-*d*₆) δ 13.65 (s, 1H), 7.64 (d, J = 9.2 Hz, 1H), 6.86 (dd, J = 9.2, 2.4 Hz, 1H), 6.63 (d, J = 2.4 Hz, 1H), 3.48 (q, J = 7.0 Hz, 4H), 1.14 (t, J = 7.0 Hz, 6H). ¹³C NMR (75 MHz, DMSO-*d*₆) δ 169.06, 162.30, 159.73, 157.27, 150.49, 132.30, 119.41, 115.42, 110.10, 101.55, 49.47, 49.47, 17.48, 17.48. HRMS (ESI) m/z: calcd for C₁₄H₁₄ClNO₄Na [M+Na]⁺, 318.0509; found 318.0509.

Synthesis of compound 4

Compound 3 (36 mg, 0.12 mmol) and NaBH₄ (6 mg, 0.16 mmol) were dissolved in 0.5 mL ethanol. The mixture was stirred at room temperature for 10 min under an argon atmosphere. The resulting colorless solution was used directly in next step without further purification.

Synthesis of compound 5

Compound 2 (60 mg, 0.2 mmol) and Et₃N (80 μL, 0.6 mmol) were dissolved in 3.0 mL of anhydrous DMF. Subsequently, compound 4 (36 mg, 0.24 mmol) was added. The reaction mixture was stirred at room temperature for 20 min. Then the mixture was poured into 100 mL water and extracted with dichloromethane (3×50 mL). The combined organic layers were washed successively with brine and water, dried over sodium sulfate, and evaporated in vacuum to leave compound 5 as an orange solid (81 mg, 98%). Mp: 158-160°C; ¹H NMR (300 MHz, CDCl₃) δ 13.24 (s, 1H), 7.52 (dd, J = 6.4, 3.0 Hz, 2H), 7.38 (d, J = 9.5 Hz, 1H), 7.33 – 7.28 (m, 3H), 6.41 (d, J = 2.6 Hz, 1H), 6.19 (dd, J = 9.5, 2.6 Hz, 1H), 3.39 (q, J = 7.1 Hz, 4H), 1.19 (t, J = 7.1 Hz, 6H). ¹³C NMR (75 MHz, CDCl₃) δ 169.19, 165.84, 163.99, 154.40, 152.47, 134.12, 133.41, 134.41, 133.30, 129.79, 129.79, 128.33, 109.88, 109.37, 106.45, 96.24, 45.02, 45.02, 12.41, 12.41. HRMS (ESI) m/z: calcd for C₂₀H₁₉NO₄SeNa [M+Na]⁺ 440.0377, found 440.0379.

Synthesis of model compound 6

To a mixture of compound 5 (83 mg, 0.2 mmol), phenol (28 mg, 0.3 mmol), EDCI (28 mg, 0.3mmol) and DMAP (4 mg, 0.03 mmol) was added dry CH₂Cl₂ (3 mL) at room temperature. The mixture was stirred at room temperature for 1 hour. Then solvent was removed under reduced pressure and the resultant residue was further purified by silica gel chromatography to afford the desired product 6 as an orange solid (56 mg, 57%). Mp: 155-156°C; ¹H NMR (600 MHz, CDCl₃) δ 7.66 (d, J = 8.9 Hz, 1H), 7.54 (d, J = 3.3 Hz, 2H), 7.38 (t, J = 7.8 Hz, 2H), 7.23 (dd, J = 15.6, 5.3 Hz, 6H), 6.49 – 6.44 (m, 2H), 3.38 (d, J = 7.0 Hz, 4H), 1.18 (t, 6H). ¹³C NMR (150 MHz, CDCl₃) δ 163.68, 157.53, 155.41, 151.61, 150.69, 147.90, 132.47, 131.24, 129.73, 129.60, 129.38, 128.00, 126.09, 121.66, 119.98, 109.43, 97.13, 44.94, 12.41. HRMS (ESI) m/z: calcd for C₂₆H₂₃NO₄SeNa [M+Na]⁺, 516.084; found 516.0693.

Synthesis of model compound 7

Compound 7 was prepared using the same procedure for compound 6. Yield: 62%. Mp: 189-190°C; ¹H NMR (600 MHz, CDCl₃) δ 7.65 (d, J = 9.0 Hz, 1H), 7.53 (dd, J = 6.2, 2.9 Hz, 2H), 7.24 (d, J = 2.7 Hz, 2H), 7.13 (d, J = 9.0 Hz, 2H), 6.88 (d, J = 9.0 Hz, 2H), 6.76 (s, 1H), 6.45 (dd, J = 12.4, 3.1 Hz, 2H), 3.79 (s, 3H), 3.38 (q, J = 7.0 Hz, 4H), 1.18 (t, J = 7.1 Hz, 6H). ¹³C NMR (150 MHz, CDCl₃) δ 164.07, 157.41, 155.40, 151.65, 144.18, 132.46, 131.20, 129.71, 129.62,

127.97, 122.41, 115.99, 114.74, 114.37, 109.99, 109.34, 108.43, 97.05, 55.58, 44.87, 12.41. HRMS (ESI) *m/z*: calcd for C₂₇H₂₅NO₃SeNa [M+Na]⁺, 546.0796; found 546.0800.

Synthesis of model compound 8

Compound **8** was prepared using the same procedure for compound **6**. Yield: 74%. Mp: 156-157°C; ¹H NMR (600 MHz, CDCl₃) δ 8.25 (d, *J* = 8.9 Hz, 2H), 7.69 (d, *J* = 9.1 Hz, 1H), 7.51 (d, *J* = 3.2 Hz, 2H), 7.32 (d, *J* = 8.9 Hz, 2H), 7.26 (d, *J* = 1.9 Hz, 3H), 6.49 (d, *J* = 7.3 Hz, 1H), 6.46 (s, 1H), 3.40 (dd, *J* = 13.8, 6.8 Hz, 4H), 1.20 (t, *J* = 7.0 Hz, 6H). ¹³C NMR (150 MHz, CDCl₃) δ 162.74, 157.47, 155.44, 155.38, 152.06, 149.83, 145.45, 132.59, 131.23, 129.82, 129.36, 128.21, 125.11, 122.57, 109.54, 108.46, 97.00, 44.96, 12.42. HRMS (ESI) *m/z*: calcd for C₂₆H₂₂N₂O₆SeNa [M+Na]⁺, 561.0535; found 561.0534.

Model reaction of compounds 6, 7 and 8 with Na₂S₂

General procedure: to the solution of compound **6** (30 mg, 0.06 mmol) in CH₃CN (1.0 mL) and PBS buffer (1.0 mL, 50 mM, pH 7.4) was added Na₂S₂ (33 mg, 0.3 mmol). The mixture was stirred for 1 hour at room temperature and then diluted with ethyl acetate (20 mL). The organic layer was separated, dried by Na₂SO₄, and concentrated. Purification by flash column chromatography afforded compound **9** as a yellow solid (13 mg, 82% yield). Mp: 201-202°C; ¹H NMR (300 MHz, CDCl₃) δ 7.57 (d, *J* = 9.1 Hz, 1H), 6.67 (dd, *J* = 9.1, 2.5 Hz, 1H), 6.49 (d, *J* = 2.5 Hz, 1H), 3.49 (q, *J* = 7.1 Hz, 4H), 1.27 (t, *J* = 7.1 Hz, 6H); ¹³C NMR (75 MHz, CDCl₃) δ 170.03, 155.56, 154.81, 153.61, 124.73, 109.77, 106.15, 105.76, 96.56, 45.25, 12.40; HRMS (ESI) *m/z*: calcd for C₁₄H₁₄NO₃S₂ [M+H]⁺ 308.0415, found 308.0414.

In the case of compound **7**, compound **9** was obtained in 80% yield.

In the case of compound **8**, compound **9** was obtained in 92% yield.

Model reaction of compounds 6, 7 and 8 with N-acetyl-cysteine methyl ester

General procedure: To the solution of compound **6** (25 mg, 0.05 mmol) in CH₃CN (1.0 mL) and PBS buffer (1.0 mL, 50 mM, pH 7.4) was added N-acetyl-cysteine methyl ester (45 mg, 0.25 mmol). The mixture was stirred for 1 hour at room temperature and then diluted with ethyl acetate (10 mL). The organic layer was separated, washed with brine (3×5 mL), dried by Na₂SO₄, and concentrated. Purification by column chromatography afforded compound **10** (25 mg, 96%). Mp: 55-56 °C; ¹H NMR (300 MHz, CDCl₃) δ 7.72 (d, *J* = 9.1 Hz, 1H), 7.53-7.43 (m, 2H), 7.37-7.31 (m, 3H), 7.10 (d, *J* = 7.5 Hz, 1H), 6.69 (dd, *J* = 9.2, 2.5 Hz, 1H), 6.52 (d, *J* = 2.5 Hz, 1H), 4.84-4.90 (m, 1H), 3.65-3.60 (m, 1H), 3.55-3.34 (m, 4H) 1.89 (s, 3H), 1.26 (t, *J* = 4.9 Hz, 6H) ¹³C NMR (75 MHz, CDCl₃) δ 170.16, 170.02, 164.48, 157.45, 155.77, 152.01, 150.85, 150.62, 129.57, 128.70, 126.43, 121.66, 118.69, 109.83, 107.19, 97.51, 53.05, 52.75, 45.04, 7.78, 29.70, 12.44. HRMS (ESI) *m/z*: calcd for C₂₆H₂₈N₂O₇SNa [M+Na]⁺ 535.1515; found 535.1519.

Compound **11** was obtained in 95% yield. ¹H NMR (300 MHz, CDCl₃) δ 7.71 (d, *J* = 9.1 Hz, 1H), 7.26 (d, *J* = 9.0 Hz, 2H), 7.10 (d, *J* = 7.7 Hz, 1H), 6.96 (d, *J* = 9.1 Hz, 2H), 6.68 (dd, *J* = 9.2, 2.4 Hz, 1H), 6.51 (d, *J* = 2.4 Hz, 1H), 4.91 – 4.86 (m, 1H), 3.84 (s, 3H), 3.81 (s, 3H), 3.69 (s, 2H), 3.45 (t, *J* =

7.1 Hz, 4H), 1.89 (s, 3H), 1.25 (t, *J* = 5.1 Hz, 6H). HRMS (ESI) *m/z*: calcd for C₂₇H₃₀N₂O₈SNa [M+Na]⁺ 565.1621; found 580.1619.

Compound **12** was obtained in 98% yield. ¹H NMR (300 MHz, CDCl₃) δ 8.36 (d, *J* = 9.1 Hz, 2H), 7.73 (d, *J* = 9.2 Hz, 1H), 7.55 (d, *J* = 9.1 Hz, 2H), 6.90 (d, *J* = 7.1 Hz, 1H), 6.71 (dd, *J* = 9.2, 2.4 Hz, 1H), 6.53 (d, *J* = 2.2 Hz, 1H), 4.93 – 4.84 (m, 1H), 3.71 (s, 3H), 3.59 (d, *J* = 3.9 Hz, 2H), 3.48 (dd, *J* = 14.1, 7.0 Hz, 4H), 1.91 (s, 3H), 1.29 (s, 6H). HRMS (ESI) *m/z*: calcd for C₂₆H₂₇N₃O₉SNa [M+Na]⁺ 580.1366; found 580.1373.

Synthesis of ACC-SePh

To a solution of compound **5** (80 mg, 0.19 mmol), compound **13** (50 mg, 0.285 mmol), EDCI (56 mg, 0.3 mmol), DMAP (2.4 mg, 0.02 mmol) was added dry CH₂Cl₂ (10 mL). The mixture was stirred for 2 h at room temperature. Then the solvent was removed under pressure and resultant crude material was purified by column chromatography to afford ACC-SePh as an orange solid (51 mg, 52% yield). Mp: 207-210°C; ¹H NMR (300 MHz, CDCl₃) δ 7.74 (d, *J* = 9.1 Hz, 1H), 7.63 (d, *J* = 8.7 Hz, 1H), 7.60 – 7.53 (m, 2H), 7.30 (dd, *J* = 5.1, 1.7 Hz, 3H), 7.24 (dd, *J* = 8.7, 2.3 Hz, 1H), 7.14 (d, *J* = 2.2 Hz, 1H), 6.54 (dd, *J* = 9.1, 2.6 Hz, 1H), 6.49 (d, *J* = 2.5 Hz, 1H), 6.29 (d, *J* = 1.2 Hz, 1H), 3.43 (q, *J* = 7.1 Hz, 4H), 2.45 (d, *J* = 1.2 Hz, 3H), 1.23 (t, *J* = 7.1 Hz, 6H). ¹³C NMR (75 MHz, CDCl₃) δ 163.03, 160.56, 157.51, 155.43, 154.10, 153.10, 151.96, 151.92, 149.43, 132.65, 131.24, 129.85, 129.34, 128.27, 125.33, 118.51, 118.26, 118.04, 114.56, 110.54, 109.65, 108.69, 97.21, 45.04, 18.76, 12.42. HRMS (ESI) *m/z*: calcd for C₃₀H₂₅NO₆SeNa [M+Na]⁺ 598.0745; found 598.0751.

RESULTS AND DISCUSSION

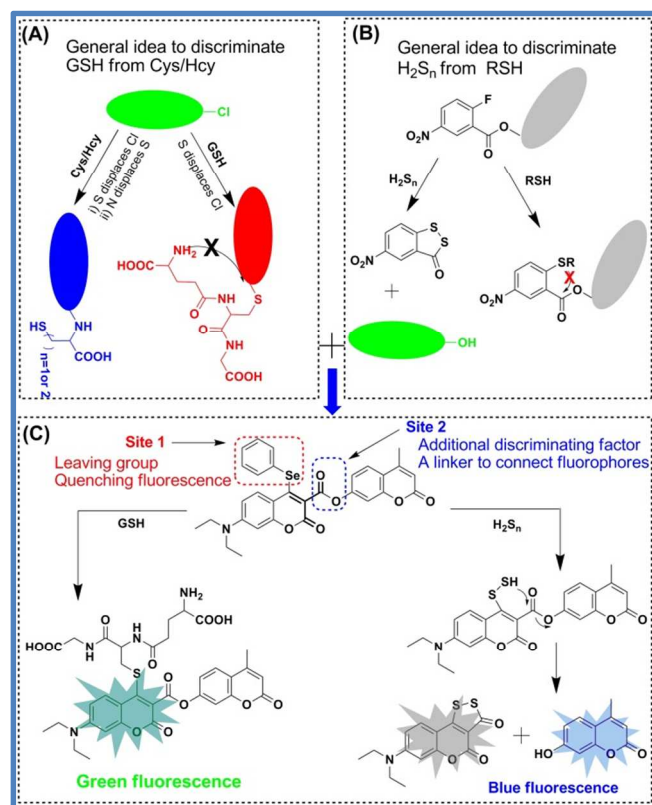
Rational design of ACC-SePh

The design strategy for ACC-SePh is depicted in Scheme 1. Combining the previously reported strategies for GSH (Scheme 1A) and H₂S_n (Scheme 1B) to a single-molecule probe through judicious structure modification may provide an effective approach to achieve the goal of simultaneously detecting GSH and H₂S_n from different emission channels. Motivated by this strategy, a novel dual-detection fluorescence probe, ACC-SePh, was rationally designed (Scheme 1C) based on the following considerations: (1) Two coumarin dyes, 7-diethylaminocoumarin and 7-hydroxycoumarin, were chosen as the fluorophores because they displayed excellent photophysical properties. Moreover, their photophysical properties can be easily tuned through delicate modification at appropriate positions.³⁶ In addition, their emission spectra were well-separated, which enable the detection of GSH and H₂S_n from different emission channels. (2) Phenylselenide moiety was selected as reaction site 1 because it functions not only as a leaving group in the S_NAr substitution reaction, but also as an effective fluorescence quencher via photo-induced electron transfer (PET) to ensure a low background signal. Furthermore, phenylselenide lies in 4-position of 7-diethylamino-coumarin moiety of ACC-SePh, which is doubly activated by two nearby carbonyl and thus is reactive.³⁷ (3) 7-Diethylaminocoumarin and 7-hydroxycoumarin were connected through simple esterification. The fluorescence of 7-hydroxycoumarin would be quenched because of the esterification. Notably, the ester group lies in 3-position (the ortho

position of phenylselenide) of 7-diethylaminocoumarin moiety, and thereby may function as an additional discriminating factor (site 2) to ensure the discrimination of H_2S_n from other RSS.

Based on the above design strategy, we anticipate that ACC-SePh could respond to GSH and H_2S_n with distinct fluorescence signals. As shown in Scheme 1C, when ACC-SePh is treated with GSH, the phenylselenide moiety would be replaced by thiol group of GSH through S_NAr substitution reaction to produce ACC-GSH. However, the reaction between H_2S_n and ACC-SePh is quite different. Initially, similar S_NAr substitution reaction between H_2S_n and ACC-SePh is expected to occur to form the corresponding intermediate ACC-SSH, and the following intermolecular cyclization between the thiol group and the adjacent ester group (site 2) would ultimately lead to the release of coumarindithiolone (**9**) and 7-hydroxycoumarin (**13**). Based on the totally different chemical structures and thus the distinct optical properties of the corresponding products ACC-GSH, **9** and **13**, simultaneous detection of GSH and H_2S_n from different emission channels through a single-molecule fluorescent probe would be promising to realize.

Scheme 1. (A) General idea to discriminate GSH from Cys/Hcy; (B) General idea to discriminate H_2S_n from RSH; (C) The design rational of novel dual detection fluorescent probe ACC-SePh for GSH and H_2S_n .

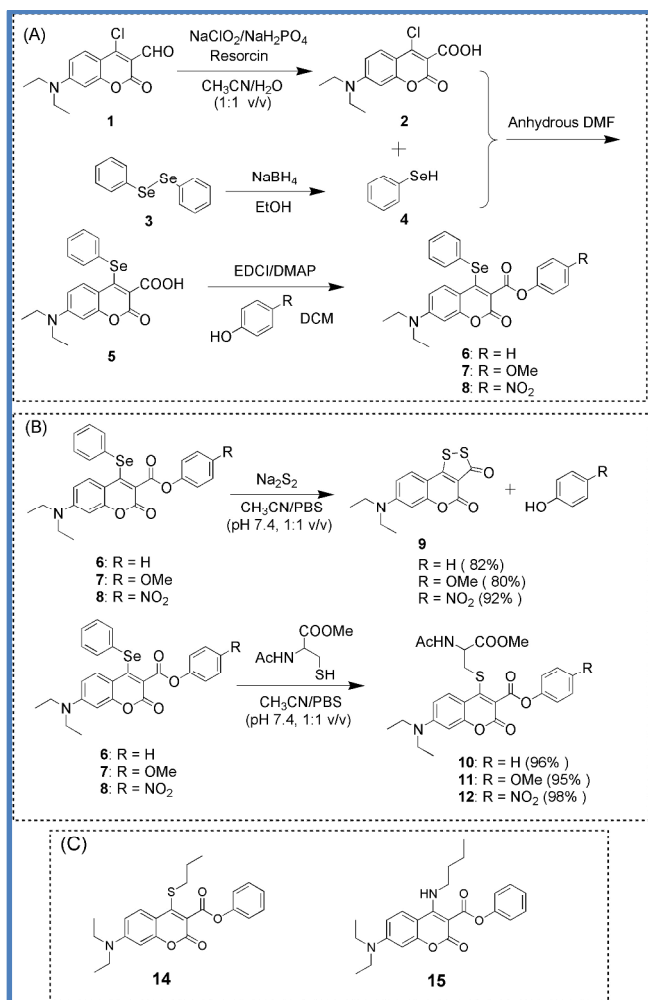


Model reaction studies

To test the above-mentioned speculation, three 4-phenylselenide-7-diethylaminocoumarin ester derivatives (**6-8**) were synthesized (Scheme 2A) as the model compounds and their reactions with Na_2S_2 (H_2S_2 maybe an active species of H_2S_n , there should be a dynamic equilibrium between H_2S_2 to other H_2S_n , therefore Na_2S_2 was selected as the primary model com-

pound of H_2S_n) or N-acetyl-cysteine methyl ester (as a GSH model) were systematically studied (Scheme 2B). All these reactions were carried out in PBS buffer (pH 7.4, 10 mM, containing 50% CH_3CN , v/v), and the relevant products were analyzed after 1 h at room temperature. As expected, when compound **6** was treated with 5.0 equivalents of Na_2S_2 , the desired cyclization product coumarindithiolone (**9**) was obtained in good yield (82%). Noteworthy, compound **9** was essentially non-fluorescent, its quantum yield was determined to be 0.0004 in PBS buffer (containing 1 mM CTAB). Moreover, both the electron-donating group (-OMe) and electron-withdrawing group (-NO₂) on the substrates (model compounds **7** and **8**) caused insignificant influences on this reaction, and the corresponding yields for **9** were identified to be 80% and 92%, respectively. Now, let us turn our attention to the reactions between model substrates and N-acetyl-cysteine methyl ester. After addition of 5.0 equivalents of N-acetyl-cysteine methyl ester to the solution of **6**, the expected substitution product **10** was obtained in 96% yield. Similar results were obtained in the cases of model compounds **7** and **8**, the corresponding yields for substitution products **11** and **12** were identified to be 95% and 98%, respectively. All these traits indicated that our proposed design strategy might be useful in developing dual-detection fluorescent probes which were capable of sensing GSH and H_2S_n simultaneously from different emission channels.

Scheme 2. (A) Synthetic route of model compounds 6-8; (B) Model reaction of the probes with H_2S_n and GSH; (C) Control compound 14-15.



Synthesize and Uv-vis spectra studies of ACC-SePh

As a proof of concept, the well-designed probe, ACC-SePh, was synthesized (Scheme 3) and its structure was fully characterized by ^1H NMR, ^{13}C NMR and HRMS (see Supporting Information). Initially, we examined the reactivity of ACC-SePh toward H_2S_n and GSH through time-dependent Uv-vis spectra in PBS buffer (10 mM, pH 7.4, containing 1mM cetyltrimethyl ammonium bromide (CTAB)) at room temperature. As shown in Figure 1a-b, ACC-SePh displayed a main absorption peak at 434 nm. Upon addition of Na_2S_2 , the absorption peak at 434 nm decreased immediately and a new peak at 355 nm emerged at the same time; after that, the absorption peak at 434 nm re-increased gradually, along with the slowly decrease of the absorption peak at 355 nm. According to the aforementioned speculation, the initial drastic absorption variation should be assigned to the rapid $\text{S}_\text{N}\text{Ar}$ displacement reaction to form the intermediate ACC-SSH. The following sluggish intermolecular cyclization would ultimately lead to the release of compound **9** and **13** (Scheme 1C), thereby causing the gradual colorimetric changes at 434 nm and 355 nm. This speculation can be supported by the absorption spectra of compound **9** and **13** under the same conditions (Figure S1). Next, let us turn our attention to GSH. As shown in Figure 1c-d, addition of GSH to the solution of ACC-SePh led to a slight increase at 434 nm, which then reached the stable absorption plateau within 2 min. According to the aforementioned speculation, this new absorption peak should be assigned to ACC-GSH, which was supported by the control

compound **14** (Figure S2). In addition, compound **9**, **13** and the adduct ACC-GSH were also observable in the corresponding HRMS titration experiments (Figure S3-S4).

Scheme 3. Synthetic route of ACC-SePh.

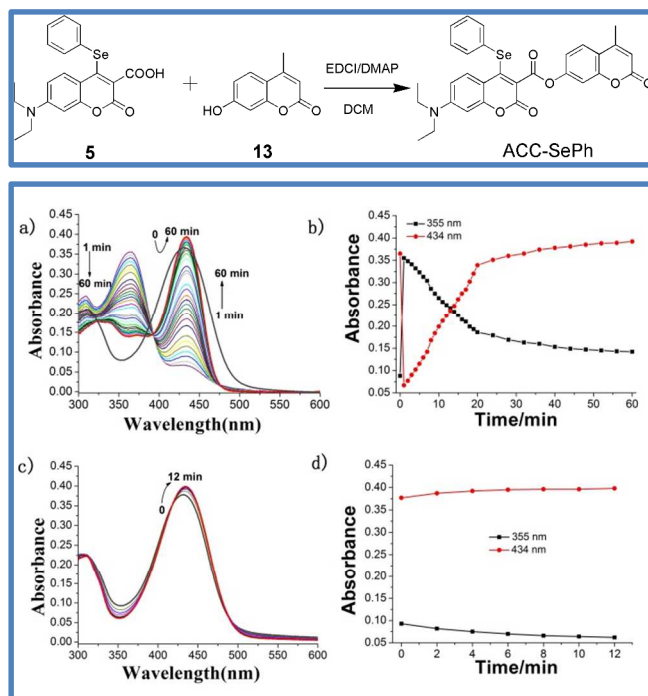
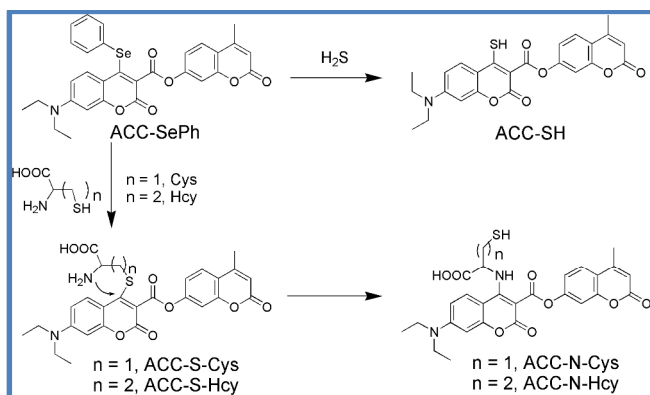


Figure 1. (a-b) Time-dependent Uv-vis spectra of ACC-SePh (10 μM) in the presence of 10 equiv of Na_2S_2 in PBS buffer (10 mM, pH 7.4, containing 1mM CTAB) (a) and the corresponding time-dependent absorption intensity changes (b); (c-d) Time-dependent Uv-vis spectra of ACC-SePh (10 μM) in the presence of 10 equiv of GSH in PBS buffer (10 mM, pH 7.4, containing 1mM CTAB) (c) and the corresponding time-dependent absorption intensity changes (d).

Subsequently, the reactivity of ACC-SePh toward other biologically abundant RSS, such as Cys, Hcy and H_2S , were also investigated through time-dependent Uv-vis spectra in PBS buffer (10 mM, pH 7.4, containing 1mM CTAB) at room temperature. Addition of Cys/Hcy to the solution of ACC-SePh, led to the decrease of the absorption peak at 434 nm, followed by a simultaneous emergence of a new peak at 375 nm (Figure S5-S6). The absorption at 375 nm should be assigned to ACC-N-Cys/ACC-N-Hcy, which was supported by the control compound **15** (Figure S7-S8). According to the well-established mechanism,^{17,37-38} Cys (or Hcy) may react with ACC-SePh through $\text{S}_\text{N}\text{Ar}$ displacement to form ACC-S-Cys (or ACC-S-Hcy), and the following intermolecular rearrangement would lead to ACC-N-Cys (or ACC-N-Hcy) (Scheme 4). On the other hand, addition of Na_2S to the solution of ACC-SePh, led to the fast decrease of the absorption peak at 434 nm, along with the simultaneous appearance of a new peak at 365 nm (Figure S9). We speculate that the absorption peak at 365 nm should be assigned to ACC-SH (Scheme 4). Unfortunately, our attempt to purify ACC-SH was unsuccessful, presumably due to the instability of ACC-SH on silica gel. Overall, the above traits are in good agreement with our proposed reaction mechanisms.

Scheme 4. Proposed reaction mechanism of ACC-SePh with H_2S and Cys/Hcy.



Fluorescence spectra studies

The emission behavior of ACC-SePh upon addition of H_2S_n and GSH were investigated in PBS buffer (10 mM, pH 7.4, containing 1mM CTAB). Firstly, we selected the main absorption peak of **13** at 366 nm as the excitation wavelength to probe H_2S_n . ACC-SePh was essentially non-fluorescent due to the effective PET process induced by phenylselenide moiety. Upon addition of Na_2S_2 , a strong emission band centered at 465 nm can be observed (Figure S10) and reached a stable intensity plateau within 60 min (Figure S11). In this case, an approximate 21-fold increase in fluorescence intensity at 465 nm can be observed. By comparison, GSH and Na_2S only elicited a 3- and 2-fold intensity enhancement at 465 nm, indicating the potential capability of ACC-SePh to detect H_2S_n over GSH and H_2S . Secondly, we selected the main absorption peak of **14** at 430 nm as the excitation wavelength to probe GSH. Under this excitation wavelength, ACC-SePh also displayed negligible fluorescence. However, upon addition of GSH, the significant fluorescence enhancement at 540 nm can be observed (Figure S12) and the intensity can reach equilibrium within 5 min (Figure S13). In this case, an approximate 16-fold increase in fluorescence intensity at 540 nm can be observed. Importantly, addition of Na_2S_2 or Na_2S can hardly elicited any significant fluorescence changes of ACC-SePh, indicative the strong capability of ACC-SePh to detect GSH over Na_2S_2 and Na_2S .

Next, we evaluated the changes in the emission spectra of ACC-SePh upon addition of incremental amounts of Na_2S_2 or GSH in PBS buffer (10 mM, pH 7.4, containing 1mM CTAB). As shown in Figure 2a, addition of incremental amounts of Na_2S_2 to the solution of ACC-SePh led to a gradual increase of the fluorescence intensity at 465 nm. Moreover, the plot of the fluorescence intensity at 465 nm versus the concentrations of Na_2S_2 exhibited good linearity ($R = 0.9914$) in the range of 0-40 μM (Figure 2b). The detection limit ($S/N = 3$) for Na_2S_2 was determined to be 40 nM. Noteworthy, other H_2S_n species, such as Na_2S_3 or Na_2S_4 , exhibited similar reactivity toward ACC-SePh (Figure S14). In the case of GSH, the fluorescence intensity at 540 nm increased linearly as the concentration of GSH up to 20 μM (Figure 2c). The corresponding detection limit was determined to be 56 nM ($S/N = 3$) (Figure 2d). Taking together, these experimental results demonstrate high sensitivity of ACC-SePh for H_2S_n and GSH, suggesting that ACC-SePh may has the potential to be used for intracellular H_2S_n or GSH monitoring.

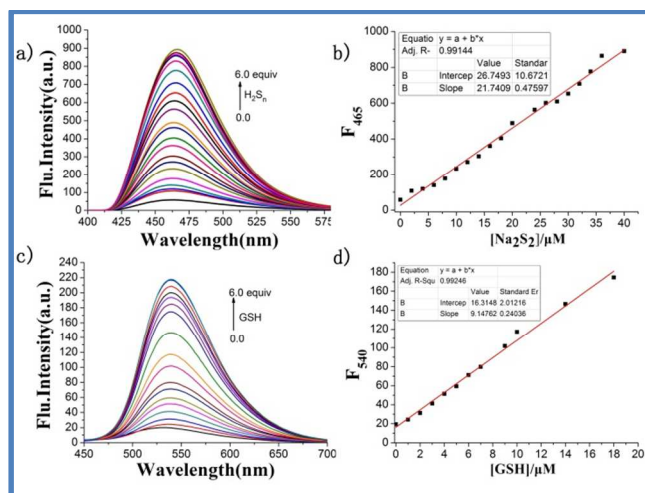


Figure 2. (a) Fluorescence spectra of ACC-SePh (10 μM) after addition of various concentrations of Na_2S_2 (0, 2, 4, 6, 8, 10, 12, 14, 16, 18, 20, 24, 26, 28, 30, 32, 34, 36, 40, 45, 50, 55, 60 μM) and (b) the corresponding linear relationship between F_{465} and Na_2S_2 concentrations (0-40 μM) ($\lambda_{\text{ex}} = 366$ nm, slits 5/5 nm); (c) Fluorescence spectra of ACC-SePh after addition of various concentrations of GSH (0, 1, 2, 3, 4, 5, 6, 7, 9, 10, 14, 18, 20, 25, 30, 40, 50, 60 μM) and (d) the corresponding linear relationship between F_{540} and GSH concentrations (0-18 μM) ($\lambda_{\text{ex}} = 430$ nm, slits 5/5 nm).

As GSH and H_2S_n may co-exist in biological systems, we wondered if the probe ACC-SePh could give effective responses when GSH and H_2S_n co-exist. As a result, the fluorescence spectra of ACC-SePh versus varying H_2S_n /GSH mixture (total sulfur concentration was fixed to be 50 μM) were studied. As the concentration of GSH seems much higher than H_2S_n in biological systems, the corresponding $[\text{H}_2\text{S}_n]/[\text{GSH}]$ ratios were installed from 0 to 1. As shown in Figure 3, following the increases of $[\text{H}_2\text{S}_n]/[\text{GSH}]$ ratios, the emission at 465 nm increased when excited at 366 nm. On the contrary, at 430 nm excitation, the emission at 540 nm decreased upon the increasing of $[\text{H}_2\text{S}_n]/[\text{GSH}]$ ratios. In addition, both F_{465} and F_{540} changed linearly with $[\text{H}_2\text{S}_n]/[\text{GSH}]$ ratios in the range of 0 to 0.42 (Figure S15-S16). These traits indicated that ACC-SePh could be used for the determination of relative H_2S_n and GSH concentrations when they co-exist.

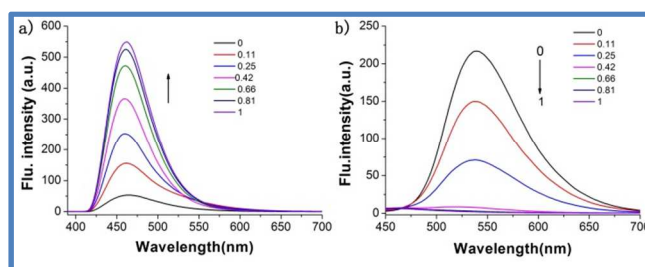


Figure 3. Fluorescence spectra of ACC-SePh (10 μM) with varying $[\text{H}_2\text{S}_n]/[\text{GSH}]$ mixture solution ($[\text{H}_2\text{S}_n]/[\text{GSH}]$ ratios were 0, 0.11, 0.25, 0.42, 0.66, 0.81, 1). (a) Excited at 366 nm, slits 5/5 nm); (b) Excited at 430 nm, slits 5/5 nm.

Selectivity and effect of pH

To evaluate the selectivity of ACC-SePh, the fluorescence spectra of ACC-SePh toward various biologically relevant species, such as KCl, CaCl_2 , ZnCl_2 , MgCl_2 , NaClO, L-Glu, L-

Ser, DL-Tyr, D-Pro, Cys, DL-Met, NaHSO₃, Na₂S₂O₃, Na₂SO₄, H₂O₂, Na₂S, Hcy, GSH, Na₂S₂, were investigated. At 366 nm excitation, ACC-SePh exhibited a limited fluorescence enhancement for various species; only Na₂S₂ elicited a significant fluorescence enhancement at 465 nm (Figure 4a, Figure S17). Noteworthy, biothiols (Cys, Hcy and GSH) also triggered a slight fluorescence enhancement of ACC-SePh at 465 nm due to the formation of blue emissive amino substituted products. These observations were consistent with the above-mentioned Uv-vis spectra results. At 430 nm excitation, only GSH caused a significant fluorescence turn-on at 540 nm, other biological species, including Cys and Hcy, triggered almost no significant fluorescence enhancement (Figure 4b, Figure S18-S19). Overall, these results demonstrate that ACC-SePh is highly selective for H₂S_n and GSH over other competitive species at different excitations.

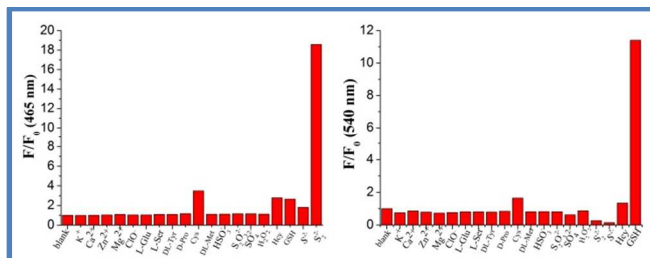


Figure 4. Fluorescence enhancement (F/F_0) of ACC-SePh (10 μ M) in the presence of 100 μ M various biological related species in PBS buffer (10 mM, pH 7.4, containing 1 mM CTAB). (a) F/F_0 at 465 nm, excited at 366 nm; (b) F/F_0 at 540 nm, excited at 430 nm.

The effect of pH on the response of ACC-SePh and its response to Na₂S₂ and GSH were also studied. As shown in Figure S20-S21, free ACC-SePh exhibited no significant fluorescence enhancement at 465 nm or 540 nm in broad pH range (1.0-9.0), indicating that ACC-SePh was stable at physiological conditions. However, under strong basic conditions (pH > 10.0), strong fluorescence at 465 nm was observed, presumably due to the fact that the ester group in ACC-SePh was hydrolyzed under these conditions to release the compound **13**. Meanwhile, at 366 nm excitation, addition of Na₂S₂ induced remarkable fluorescence enhancement at 465 nm in the pH range 6.0-9.0. At 430 nm excitation, addition of GSH induced significant fluorescence enhancement at 540 nm in the pH range 7.0-11.0. All these results suggested that ACC-SePh can function properly in biological environments.

Cell imaging

Encouraged by the excellent sensing properties of the probe in aqueous solution, we further evaluated the capability of ACC-SePh to selectively sense H₂S_n and GSH in living cells. As shown in Figure 5, when RAW264.7 cells were incubated with ACC-SePh for 30 min, they gave weak fluorescence in blue channel and strong fluorescence in green channel (Figure 5A1-A2), indicating that ACC-SePh is responsive to intracellular GSH. When RAW264.7 cells were pretreated with 50 μ M Na₂S₂ for 15 min and then further incubated with ACC-SePh, a significant increase in blue channel and a marked decrease in green channel can be observed (Figure 5B1-B2). In control experiments, cells were pretreated with 1 mM *N*-ethylmaleimide (NEM, a scavenger of GSH)³⁹ for 15 min and then incubated with ACC-SePh for 30 min, no obvious fluorescence in both blue and green channels were observed (Figure 5C1-C2). These results indicate that ACC-SePh is cell-

permeable and can be used for sensing intracellular H₂S_n and GSH simultaneously from different emission channels. In addition, the MTT assay for ACC-SePh was also conducted, and the results showed that ACC-SePh has minimal cytotoxicity (Figure S22), thereby holding great potential for biological applications.

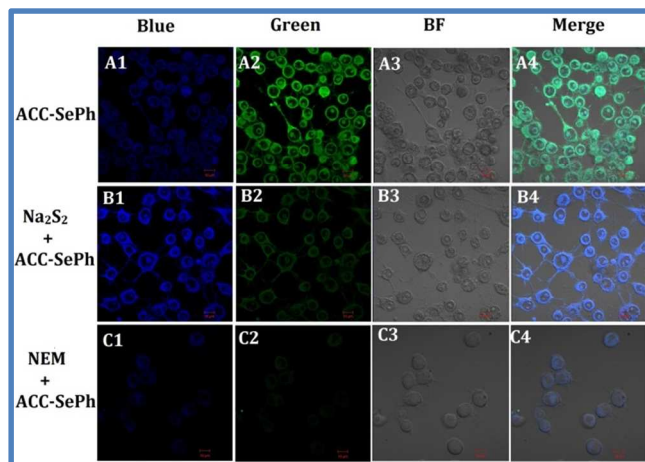


Figure 5. Confocal microscopic images of GSH and H₂S_n in living RAW264.7 cells. (A1-A4) RAW264.7 cells incubated with 5 μ M ACC-SePh and CTAB (0.5 mM); (B1-B4) RAW264.7 cells pretreated with 25 μ M Na₂S₂ and then incubated with 5 μ M ACC-SePh and CTAB (0.5 mM); (C1-C4) RAW264.7 cells pretreated with 1mM NEM and then incubated with 5 μ M ACC-SePh and CTAB (0.5 mM). Excitation wavelength: 405 nm. Emissions were collected at 450-470 nm for blue channel and 540-560 nm for green channel. Scale bar: 10 μ m.

For a further biological study, we investigate whether ACC-SePh can be used for the detection of endogenously produced H₂S_n. According to the literature, endogenous H₂S_n can be biosynthesized from cystine through cystathionine- γ -lyase (CSE).¹⁰ Therefore we sought to determine whether ACC-SePh could detect endogenous H₂S_n that was derived from cystine and CSE in living RAW264.7 cells. Initially, RAW264.7 cells were stimulated with 1 μ g/mL lipopolysaccharide (LPS) (a compound can induce the CSE mRNA in RAW264.7 cells overexpressed⁴⁰) for 8 hours. Then, cells were incubated with 1 mM NEM for 15 min to diminish the interference caused by intracellular GSH. Next, cells were incubated with 200 μ M cystine for 30 min. Finally, cells were incubated with ACC-SePh for additional 30 min. As shown in Figure 6A1-A2, strong fluorescence in blue channel and weak fluorescence in green channel can be observed. In control experiment, cells were incubated with NEM (1 mM), cystine (200 μ M), and ACC-SePh successively, only weak fluorescence in both blue channel and green channel can be observed (Figure 6B1-B2). These results demonstrated that ACC-SePh was capable of detecting endogenous H₂S_n in RAW264.7 cells.

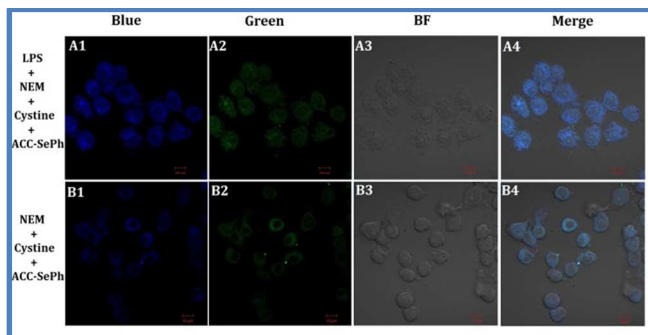


Figure 6. Confocal microscopic images of endogeneously produced H_2S_n in living RAW264.7 cells. (A1-A4) RAW264.7 cells incubated with $1 \mu\text{g/mL}$ LPS for 8 hours and then 1 mM NEM for 15 min, $200 \mu\text{M}$ cystine for 30 min, and finally incubated with $5 \mu\text{M}$ ACC-SePh and CTAB (0.5 mM) for additional 30 min; (B1-B4) RAW264.7 cells pretreated with 1 mM NEM for 15 min, $200 \mu\text{M}$ cystine for 30 min and then incubated with $5 \mu\text{M}$ ACC-SePh and CTAB (0.5 mM) for additional 30 min. Excitation wavelength: 405 nm . Emissions were collected at $450\text{--}470 \text{ nm}$ for blue channel and $540\text{--}560 \text{ nm}$ for green channel. Scale bar: $10 \mu\text{m}$.

CONCLUSIONS

In summary, we have presented in this study the rational design, synthesis, and evaluation of the first dual-detection fluorescent probe ACC-SePh that can selectively sense H_2S_n and GSH from different emission channels (H_2S_n : $\lambda_{\text{ex/em}} = 366/465 \text{ nm}$ with an approximate 21-fold increase in fluorescence intensity at 465 nm ; GSH: $\lambda_{\text{ex/em}} = 430/540 \text{ nm}$ with an approximate 16-fold increase in fluorescence intensity at 540 nm) based on the different reaction processes between ACC-SePh and common RSS (e.g. H_2S , H_2S_n , Cys/Hcy, and GSH). Preliminary biological experiments have indicated ACC-SePh could simultaneously monitor intracellular H_2S_n and GSH in living RAW264.7 cells. In addition, ACC-SePh can also be used for sensing endogenously produced H_2S_n . We hope this novel strategy could open up an avenue to develop new systems for RSS discrimination.

ASSOCIATED CONTENT

Supporting Information

Experimental details and additional spectroscopy data ^1H NMR, ^{13}C NMR and HRMS spectra of the products

The Supporting Information is available free of charge on the ACS Publications website.

AUTHOR INFORMATION

Notes

The authors declare no competing financial interest.

ACKNOWLEDGMENT

This work was supported by the Guangxi Natural Science Foundation (2016GXNSFBA380229), "BAGUI Scholar" program of Guangxi Province of China and Graduate Innovation Training Program of Guangxi Province (YCSW2017189).

REFERENCES

- (1) Paulsen, C. E.; Carroll, K. S. *Chem. Rev.* **2013**, *113*, 4633-4679.
- (2) Giles, G. I.; Jacob, C. *Biol. Chem.* **2002**, *383*, 375-388.

- (3) Giles, G. I.; Tasker, K. M.; Jacob, C. *Free Radical Biol. Med.* **2001**, *31*, 1279-1283.
- (4) Meister, A. *J. Biol. Chem.* **1988**, *263*, 17205-17208.
- (5) Hwang, C.; Sinskey, A. J.; Lodish, H. F.; *Science* **1992**, *257*, 1496-1501.
- (6) Meister, A.; Anderson, M. E.; *Annu. Rev. Biochem.* **1983**, *52*, 711-760.
- (7) Lu, S. C. *Mol. Aspects Med.* **2009**, *30*, 42-59.
- (8) Townsend, D. M.; Tew, K. D.; Tapiero, H. *Biomed. Pharmacother.* **2003**, *57*, 145-155.
- (9) Greiner, R.; Pálincás, Z.; Bäsell, K.; Becher, D.; Antelmann, H.; Nagy, P.; Dick, T. P. *Antioxid. Redox Signal.* **2013**, *19*, 1749-1765.
- (10) Ono, K.; Akaike, T.; Sawa, T.; Kumagai, Y.; Wink, D.; Tantillo, D. J.; Hobbs, A. J.; Nagy, P.; Xian, M.; Lin, J.; Fukuto, J. M. *Free Radical Biol. Med.* **2014**, *77*, 82-94.
- (11) Estevam, E. C.; Faulstich, L.; Griffin, S.; Burkholz, T.; Jacob, C. *Curr. Org. Chem.* **2016**, *20*, 211-217.
- (12) Kimura, H. *Antioxid. Redox Signal.* **2015**, *22*, 362-376.
- (13) Mishanina, T. V.; Libiad, M.; Banerjee, R. *Nat. Chem. Biol.* **2015**, *11*, 457-464.
- (14) Chen, X.; Zhou, Y.; Peng, X.; Yoon, J. *Chem. Soc. Rev.* **2010**, *39*, 2120-2135.
- (15) Lin, V. S.; Chen, W.; Xian, M.; Chang, C. J. *Chem. Soc. Rev.* **2015**, *44*, 4596-4618.
- (16) Sun, W.; Guo, S.; Hu, C.; Fan, J.; Peng, X. *Chem. Rev.* **2016**, *116*, 7768-7817.
- (17) Niu, L.-Y.; Guan, Y. -S.; Chen, Y. -Z.; Wu, L. -Z.; Tung, C. -H.; Yang, Q. -Z. *J. Am. Chem. Soc.* **2012**, *134*, 18928-18931.
- (18) Liu, C.; Chen, W.; Shi, W.; Peng, B.; Zhao, Y.; Ma, H.; Xian, M. *J. Am. Soc. Chem.* **2014**, *136*, 7257-7260.
- (19) Gao, M.; Yu, F.; Chen, H.; Chen, L. *Anal. Chem.* **2015**, *87*, 3631-3638.
- (20) Yu, F.; Gao, M.; Li, M.; Chen, L. *Biomaterials* **2015**, *63*, 93-101.
- (21) Zeng, L.; Chen, S.; Xia, T.; Hu, W.; Li, C.; Liu, Z. *Anal. Chem.* **2015**, *87*, 3004-3010.
- (22) Shang, H.; Chen, H.; Tang, Y.; Guo, R.; Lin, W. *Sens. Actuators B Chem.* **2016**, *230*, 773-778.
- (23) Gao, M.; Wang, R.; Yu, F.; You, J.; Chen, L. *Analyst* **2015**, *140*, 3766-3772.
- (24) Zhang, J.; Zhu, X. -Y.; Hu, X. -X.; Liu, H. -W.; Li, J.; Feng, L. -L.; Yin, X.; Zhang, X. -B. *Anal. Chem.* **2016**, *88*, 11892-11899.
- (25) Han, Q.; Mou, Z.; Wang, H.; Tang, X.; Dong, Z.; Wang, L.; Dong, X.; Liu, W. *Anal. Chem.* **2016**, *88*, 7206-7212.
- (26) Ma, J.; Fan, J.; Li, H.; Yao, Q.; Xu, F.; Wang, J.; Peng, X. *J. Mater. Chem. B* **2017**, *5*, 2574-2579.
- (27) Fang, Y.; Chen, W.; Shi, W.; Li, H.; Xian, M.; Ma, H.; *Chem. Commun.* **2017**, *53*, 8759-8762.
- (28) Li, K.; Chen, F.; Yin, Q.; Zhang, S.; Shi, W.; Han, D.; *Sens. Actuators B Chem.* **2018**, *254*, 222-226.
- (29) Chen, W.; Rosser, E. W.; Matsunaga, T.; Pacheco, A.; Akaike, T.; Xian, M. *Angew. Chem., Int. Ed.* **2015**, *54*, 13961-13965.
- (30) Chen, W.; Pacheco, A.; Takano, Y.; Day, J. J.; Hanaoka, K.; Xian, M. *Angew. Chem. Int. Ed.* **2016**, *55*, 9993-9996.
- (31) Yadav, P. K.; Martinov, M.; Vitvitsky, V.; Seravalli, J.; Wedmann, R.; Filipovic, M. R.; Banerjee, R. *J. Am. Chem. Soc.* **2016**, *138*, 289-299.
- (32) Ida, T.; Sawa, T.; Ihara, H.; Tsuchiya, Y.; Watanabe, Y.; Kumagai, Y.; Suematsu, M.; Motohashi, H.; Fujii, S.; Matsunaga, T.; Yamamoto, M.; Ono, K.; Devarie-Baez, N. O.; Xian, M.; Fukuto, J. M.; Akaike, T. *Proc. Natl. Acad. Sci. USA* **2014**, *111*, 7606-7611.
- (33) She, X. -P.; Song, X. -G.; He, J. -M. *Acta. Botanica. Sinica* **2004**, *46*, 1292-1300.
- (34) Sartoretto, J. L.; Kalwa, H.; Pluth, M. D.; Lippard, S. J.; Michel, T. *Proc. Natl. Acad. Sci. USA* **2011**, *108*, 15792-15797.
- (35) Komatsu, H.; Miki, T.; Citterio, D.; Kubota, T.; Shindo, Y.; Kitamura, Y.; Oka, K.; Suzuki, K. *J. Am. Chem. Soc.* **2005**, *127*, 10798-10799.
- (36) Sanghi, S.; Mohan, D.; Singh, R. D. *Asian J. Phys.* **1995**, *4*, 283-288.

(37) Kim, Y.; Mulay, S. V.; Choi, M.; Yu, S. B.; Jon, S.; Churchill, D. G. *Chem. Sci.* **2015**, *6*, 5435-5439.

(8) Liu, J.; Sun, Y. -Q.; Huo, Y.; Zhang, H.; Wang, L.; Zhang, P.; Song, D.; Shi, Y.; Guo, W. *J. Am. Chem. Soc.* **2014**, *136*, 574-577.

(39) Yellaturu, C. R.; Bhanoori, M.; Neeli, I.; Rao, G. N. *J. Biol. Chem.* **2002**, *277*, 40148-40155.

(40) Zhu, X.; Liu, S.; Liu, Y.; Wang, S.; Ni, X. *Cell. Mol. Life Sci.*, **2010**, *67*, 1119-1132.

For TOC only

